Article

Photoactive Peptides for Light-Initiated Tyrosyl Radical Generation and Transport into Ribonucleotide Reductase

Steven Y. Reece, Mohammad R. Seyedsayamdost, JoAnne Stubbe, and Daniel G. Nocera

J. Am. Chem. Soc., **2007**, 129 (27), 8500-8509• DOI: 10.1021/ja0704434 • Publication Date (Web): 14 June 2007

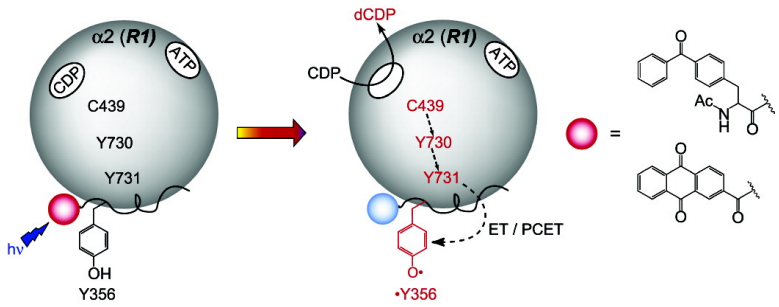

More About This Article

Additional resources and features associated with this article are available within the HTML version:

- Supporting Information
- Links to the 4 articles that cite this article, as of the time of this article download
- Access to high resolution figures
- Links to articles and content related to this article
- Copyright permission to reproduce figures and/or text from this article

View the Full Text HTML

J|A|C|S
ARTICLES
Published on Web 06/14/2007

Photoactive Peptides for Light-Initiated Tyrosyl Radical Generation and Transport into Ribonucleotide Reductase

Steven Y. Reece,[†] Mohammad R. Seyedsayamdost,[†] JoAnne Stubbe,*[,†,‡] and Daniel G. Nocera*[,†]

Contribution from the Departments of Chemistry and Biology, Massachusetts Institute of Technology, 77 Massachusetts Avenue, Cambridge, Massachusetts 02139-4307

Received January 20, 2007; E-mail: stubbe@mit.edu; nocera@mit.edu

Abstract: The mechanism of radical transport in the α2 (R1) subunit of class I *E. coli* ribonucleotide reductase (RNR) has been investigated by the phototriggered generation of a tyrosyl radical, •Y356, on a 20-mer peptide bound to α2. This peptide, Y-R2C19, is identical to the C-terminal peptide tail of the β2 (R2) subunit and is a known competitive inhibitor of binding of the native β2 protein to α2. •Y356 radical initiation is prompted by excitation ($\lambda \geq 300$ nm) of a proximal anthraquinone, Anq, or benzophenone, BPA, chromophore on the peptide. Transient absorption spectroscopy has been employed to kinetically characterize the radical-producing step by time resolving the semiquinone anion (Anq•⁻), ketyl radical (•-BPA), and Y• photoproducts on (i) BPA-Y and Anq-Y dipeptides and (ii) BPA/Anq-Y-R2C19 peptides. Light-initiated, single-turnover assays have been carried out with the peptide/α2 complex in the presence of [^{14}C]-labeled cytidine 5′-diphosphate substrate and ATP allosteric effector. We show that both the Anq- and BPA-containing peptides are competent in deoxycytidine diphosphate formation and turnover occurs via Y731 to Y730 to C439 pathway-dependent radical transport in α2. Experiments with the Y730F mutant exclude a direct superexchange mechanism between C439 and Y731 and are consistent with a PCET model for radical transport in which there is a unidirectional transport of the electron and proton transport among residues of α2.

Introduction

Correlated electron and proton motion is exquisitely controlled and utilized in biology for energy conversion.[1] Whether the electron and proton are indirectly coupled, such as they are for proton pumping across a membrane driven by electron transfer,[2,3] or intimately coupled, as they are for amino acid radical initiation and transport,[4] the precise mechanism by which Nature has fine-tuned proton-coupled electron transfer (PCET) to achieve such remarkable reactivity remains largely undefined.[5−8] To better understand this coupling mechanism by PCET in natural systems, our efforts have turned to the ∼35 Å radical transport pathway in class I *E. coli* ribonucleotide reductase (RNR).

RNR plays a crucial role in DNA replication and repair by catalyzing the reduction of nucleoside diphosphates (NDPs) to deoxynucleoside diphosphates (dNDPs).[9−11] The class I *E. coli* enzyme is composed of two homodimeric subunits designated α2 and β2, and a complex between the two is required for activity.[12] α2 houses the binding sites for the substrates and effectors, which control the specificity and rate of nucleotide reduction.[13−15] β2 harbors the diferric tyrosyl radical (•Y122) cofactor proposed to initiate nucleotide reduction by generating a transient thiyl radical (•C439) in the active site of α2.[16] The crystal structures of both α2 and β2 have been solved independently,[17−19] and a docking model of the two proteins has been proposed[17] that places Y122 on β2 at a distance >35 Å away from the C439 residue on α2. Recent PELDOR studies provide support for a long-distance radical migration.[20] Radical transport has been proposed to occur via a radical hopping mechanism involving the aromatic amino acid radical intermediates shown in Figure 1.[1,4] Specifically, the radical is proposed to hop from •Y122 → W48 → Y356 in β2 to Y731 → Y730 →

[†] Department of Chemistry.
[‡] Department of Biology.

(1) Reece, S. Y.; Hodgkiss, J. M.; Stubbe, J.; Nocera, D. G. *Philos. Trans. R. Soc., Ser. B* **2006**, *361*, 1351.
(2) Mitchell, P. *Annu. Rev. Biochem.* **1977**, *46*, 996.
(3) Williams, R. J. P. *Annu. Rev. Biophys. Biophys. Chem.* **1988**, *17*, 71.
(4) Stubbe, J.; Nocera, D. G.; Yee, C. S.; Chang, M. C. Y. *Chem. Rev.* **2003**, *103*, 2167.
(5) Cukier, R. I.; Nocera, D. G. *Annu. Rev. Phys. Chem.* **1998**, *49*, 337.
(6) Chang, C. J.; Chang, M. C. Y.; Damrauer, N. H.; Nocera, D. G. *Biophys. Biochim. Acta* **2004**, *1655*, 13.
(7) Hodgkiss, J. M.; Damrauer, N. H.; Pressé, S.; Rosenthal, J.; Nocera, D. G. *J. Phys. Chem. B* **2005**, *110*, 18853.
(8) Hammes-Schiffer, S. *Acc. Chem. Res.* **2006**, *39*, 93.
(9) Stubbe, J.; van der Donk, W. A. *Chem. Rev.* **1998**, *98*, 705.
(10) Jordan, A.; Reichard, P. *Annu. Rev. Biochem.* **1998**, *67*, 71.
(11) Stubbe, J. *Chem. Commun.* **2003**, 2511.
(12) Thelander, L. *J. Biol. Chem.* **1973**, *248*, 4591.
(13) Thelander, L.; Reichard, P. *Annu. Rev. Biochem.* **1979**, *48*, 133.
(14) Kashlan, O. B.; Scott, C. P.; Lear, J. D.; Cooperman, B. S. *Biochemistry* **2002**, *41*, 462.
(15) Kashlan, O. B.; Cooperman, B. S. *Biochemistry* **2003**, *42*, 1696.
(16) Stubbe, J.; Riggs-Gelasco, P. *Trends Biochem. Sci.* **1998**, *23*, 438.
(17) Uhlin, U.; Eklund, H. *Nature* **1994**, *370*, 533.
(18) Nordlund, P.; Sjöberg, B.-M.; Eklund, H. *Nature* **1990**, *345*, 593.
(19) Högbom, M.; Galander, M.; Andersson, M.; Kolberg, M.; Hofbauer, W.; Lassmann, G.; Nordlund, P.; Lendzian, F. *Proc. Natl. Acad. Sci. U.S.A.* **2003**, *100*, 3209.
(20) Bennati, M.; Robblee, J. H.; Mugnaini, V.; Stubbe, J.; Freed, J. H.; Borbat, P. *J. Am. Chem. Soc.* **2005**, *127*, 15014.

10.1021/ja0704434 CCC: $37.00

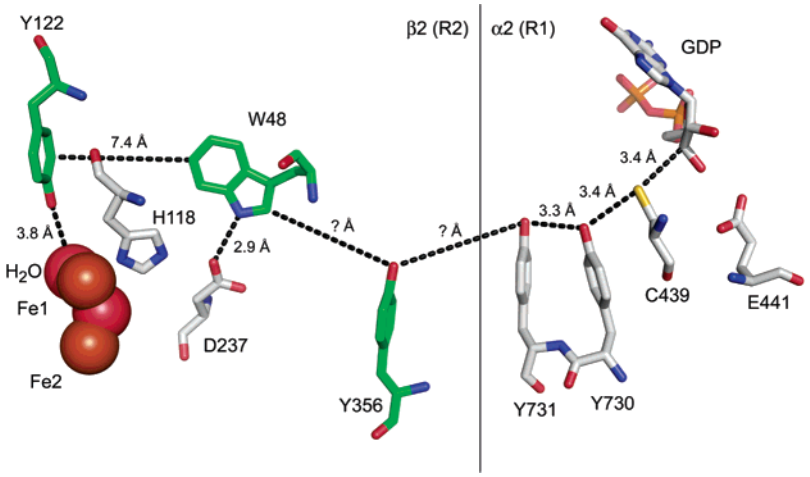

Figure 1. Conserved residues of class I RNR that compose the putative PCET pathway for radical transport from •Y122 in β2 to C439 in the α2 active site. Distances are from the separate crystal structures of the $\alpha 2^{17}$ and $\beta 2^{19}$ subunit from the *E. coli* enzyme. Residues where the radical has been directly observed or trapped via site-specific replacement with non-natural amino acid analogues are highlighted in green.[4,22] Y356 is not located in either the β2 or the α2 crystal structures; hence, its distance from W48 and Y731 is unknown.

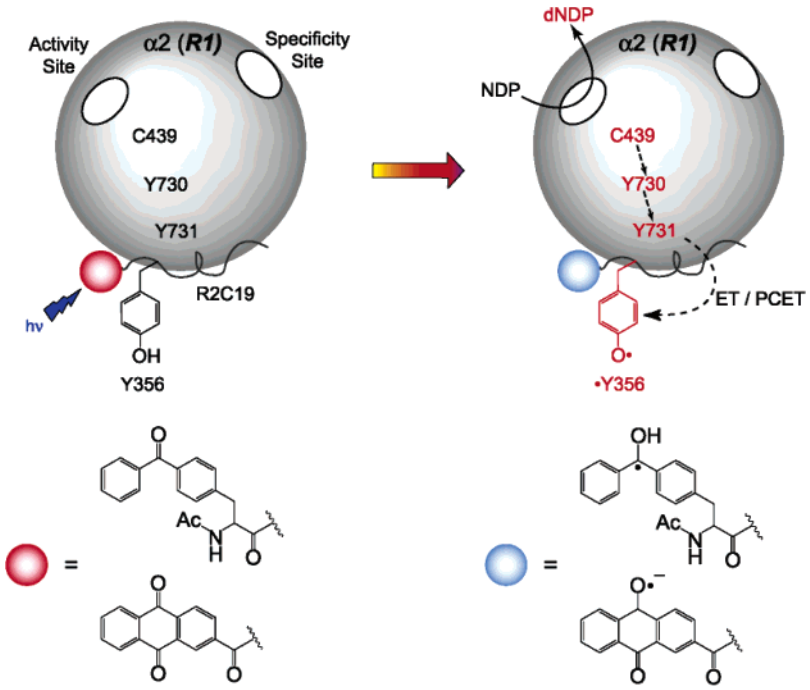

Figure 2. Experimental design for studying the kinetics of radical transport along •Y356 → Y731 → Y730 → C439 pathway. •Y356 is generated photochemically by a proximal photo-oxidant (red circle) on the R2C19 peptide. NDP, nucleoside diphosphate substrate; dNDP, deoxynucleoside diphosphate product; R2C19, 19-mer C-terminal peptide tail of β2.

C439 in α2. Under physiological conditions, oxidation of these residues requires loss of both a proton and an electron, implicating PCET[4−6] as the radical transport mechanism. Recently the first positive evidence that Y356 is a redox-active amino acid on the pathway has been presented[21] along with trapping of the radical at position 356 using the non-natural DOPA amino acid.[22] Notwithstanding, sampling of a kinetically competent intermediate[23−25]along a conformationally gated reaction profile presents a challenge to directly detecting amino acid radical intermediates.[26]

To address the challenge of kinetically resolving radical transport we simplified the RNR construct by focusing on the radical transport in the α2 subunit with the approach depicted in Figure 2. Using solid-phase peptide synthesis, we assembled the α2 binding determinant of β2, the 19-mer C-terminal peptide tail (R2C19), containing the redox-active Y356 (Y-R2C19).[27,28] A photo-oxidant, appended proximate to Y356 (Figure 2, red circle), can be photoexcited to produce •Y356, which can then be translated into the C439 active site of α2. We established

(21) Seyedsayamdost, M. R.; Yee, C. S.; Reece, S. Y.; Nocera, D. G.; Stubbe, J. *J. Am. Chem. Soc.* **2006**, *128*, 1562.
(22) Seyedsayamdost, M. R.; Stubbe, J. *J. Am. Chem. Soc.* **2006**, *128*, 2522.
(23) Hammes-Schiffer, S.; Benkovic, S. J. *Annu. Rev. Biochem.* **2006**, *75*, 519.
(24) Klinman, J. P. *Philos. Trans. R. Soc., Ser. B* **2006**, *361*, 1323.
(25) Bitetti-Putzer, R.; Dinner, A. R.; Yang, W.; Karplus, M. *J. Chem. Phys.* **2006**, *124*, 174901.
(26) Ge, J.; Yu, G.; Ator, M. A.; Stubbe, J. *Biochemistry* **2003**, *42*, 10071.
(27) Climent, I.; Sjöberg, B.-M.; Huang, C. Y. *Biochemistry* **1991**, *30*, 5164.
(28) Climent, I.; Sjöberg, B.-M.; Huang, C. Y. *Biochemistry* **1992**, *31*, 4801.

the competency of this construct using tryptophan as the phototrigger of •Y356.[29] Studies on W−Y dipeptides show that photoionization of W with UV light ($\lambda < 290$ nm) irreversibly generates W•, which in turn oxidizes Y within the pH range relevant to RNR.[30] Excitation of the peptide-α2 complex in the presence of CDP substrate and ATP effector results in dCDP formation, demonstrating enzymatic activity is retained when the entire β2 subunit is replaced by a photoactive peptide.[29] However, a significant drawback with tryptophan-based peptide constructs arises from the need for UV light to excite the tryptophan. Deep UV excitation profiles fall within the absorption envelope of RNR, thus presenting a significant problem for direct kinetic analysis of α2-bound peptides owing to innerfilter optical effects and protein instability.

Described herein is the development of peptide-based photo-oxidants of tyrosine that may be excited to the red spectral side of the protein absorption manifold. We had previous success using amino acid model systems in which tyrosine is photo-oxidized by the MLCT excited states of Re(I) complexes, which absorb in the visible spectral region.[31] However, this model is not easily adapted to RNR investigations because the facile photo-oxidation of tyrosine requires deprotonation of the phenol with p$K_a = 10$ (in order to avoid the thermodynamic barrier[32,33] confronting formation of the protonated radical cation), and α2 is stable only to pH 8.5. Tyrosine oxidation can be expedited by forming a hydrogen bond between the phenol and a base,[34−35] thus switching the photo-oxidation from ET to PCET.[37] Following this lead, we sought to develop photo-oxidants that could fulfill the dual role of electron and proton acceptor for the rapid tyrosine oxidation required in phototriggering RNR and at the same time be excited by light outside the RNR absorption manifold.

Both benzophenone and anthraquinone are strong triplet nπ* excited-state oxidants with the ability to oxidize amines, aliphatic alcohols, and even water, though sluggishly.[38−42] Studies on the mechanism of phenol oxidation by carbonyl triplet excited states have resulted in a model wherein PCET occurs within a hydrogen-bonded exciplex.[43] In this model, electron transfer from the phenol to the electronically excited carbonyl is kinetically coupled to proton transfer between the oxygen atoms of phenol and the photo-oxidant. We now report that excitation

Chart 1

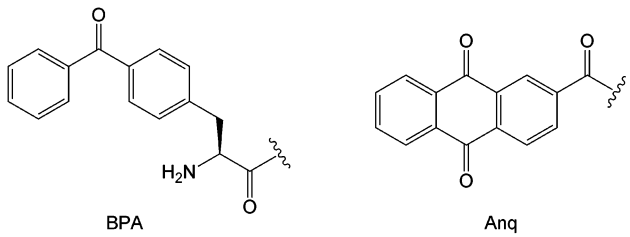

of the benzophenone unnatural amino acid (BPA) or Anq chromophore (Anq) (see Chart 1) appended to the N-terminus of the Y-R2C19 peptide generates Y•. The kinetics for the time evolution of the radical has been investigated with transient absorption (TA) spectroscopy. The (•BPA/•Anq$^-$)−Y• diradical on the R2C19 peptide is generated in the subnanosecond time scale at pH 7.5 and with excitation light of $\lambda > 300-355$ nm. We also show that these peptides bind to α2 and induce dCDP formation upon excitation of the peptide-α2 complex. Mutation of Y730 to F in α2 inhibits RNR turnover, consistent with a PCET model for radical transport in α2 in which the proton and electron transfer along a unidirectional pathway within α2.

Experimental Section

Materials. Anthraquinone-2-carboxylic acid (Anq-COOH), reduced β-nicotinamide adenine dinucleotide phosphate (NADPH), *N*-hydroxyurea, deoxycytidine (dC), cytidine-5′-diphosphate (CDP), trifluoroacetic acid (TFA), adenosine 5′-triphosphate (ATP), 1-(3-dimethylaminopropyl)-3-ethylcarbodiimide hydrochloride (EDC•HCl), piperidine, diisopropylethylamine (DIPEA), triisopropylsilane, and *N*-methylmorpholine (NMM) were purchased from Sigma-Aldrich. 4-Benzoyl-*N*-[(9*H*-fluoren-9-ylmethoxy)carbonyl]-L-phenylalanine (Fmoc-BPA-COOH) and l-phenylalanine *tert*-butyl ester hydrochloride (F-O*t*Bu•HCl) were from Advanced ChemTech. 1-Hydroxybenzotriazole (HOBt) and L-tyrosine *tert*-butyl ester (Y-O*t*Bu) were obtained from NovaBiochem. *O*-(7-Azobenzotriazol-1-yl)-1,1,3,3-tetramethyluronium hexafluorophosphate (HATU), *O*-(1,1-dimethylethyl)-*N*-[(9*H*-fluoren-9-ylmethoxy)carbonyl]-L-tyrosine (Fmoc-Y(*t*Bu)-OH), and *N*-[(9*H*-fluoren-9-ylmethoxy)-carbonyl]-L-phenylalanine (Fmoc-F-OH) were purchased from Applied Biosystems. [2-^{14}C]-CDP was purchased from Moravek Biochemicals and diluted to a specific activity of 5455 cpm/nmol. Calf-intestine alkaline phosphatase (20 U/μL) was purchased from Roche. All chemicals were used as received except for piperidine, which was freshly distilled from KOH under N_2 prior to use. 4-Benzoyl-L-phenylalanyl-tyrosine methyl ester trifluoroacetic acid (BPA-Y-OMe•TFA) was available from a previous study.[44] *E. coli* thioredoxin (TR, SA of 40 U/mg), *E. coli* thioredoxin reductase (TRR, SA of 1800 U/mg), and *E. coli* β2 (SA of 6800 nmol/min mg) were isolated as previously described.[45]

***N*-[(9,10-Dihydro-9,10-dioxo-2-anthracenyl)carbonyl]-L-tyrosine (Anq-Y-OH).** Anq-COOH (300 mg, 1.19 mmol, 1.0 equiv), Y-O*t*Bu (282 mg, 1.0 equiv), EDC•HCl (250 mg, 1.1 equiv), and HOBt (177 mg, 1.1 equiv) were combined in a 100 mL flask with 30 mL of DMF. NMM (530 μL, 4.0 equiv) was added, and the solution was stirred overnight. The solvent was removed in vacuo, and the resulting oil was dissolved in 80 mL of methylene chloride. The organics were washed with 2 × 50 mL of water, dried over $MgSO_4$, and filtered to remove the drying agent. The solvent was removed in vacuo to yield a yellow oil, which was dissolved in a few milliliters of methylene

(29) Chang, M. C. Y.; Yee, C. S.; Stubbe, J.; Nocera, D. G. *Proc. Natl. Acad. Sci. U.S.A.* **2004**, *101*, 6882.
(30) Reece, S. Y.; Stubbe, J. S.; Nocera, D. G. *Biochim. Biophys. Acta* **2005**, *1706*, 232.
(31) Reece, S. Y.; Nocera, D. G. *J. Am. Chem. Soc.* **2005**, *127*, 9448.
(32) Mayer, J. M. *Annu. Rev. Phys. Chem.* **2004**, *55*, 363.
(33) Sjödin, M.; Styring, S.; Wolpher, H.; Xu, Y.; Sun, L.; Hammarström, L. *J. Am. Chem. Soc.* **2005**, *127*, 3855.
(34) Rhile, I. J.; Markle, T. F.; Nagao, H.; DiPasquale, A. G.; Lam, O. P.; Lockwood, M. A.; Rotter, K.; Mayer, J. M. *J. Am. Chem. Soc.* **2006**, *128*, 6075.
(35) Fecenko, C. J.; Meyer, T. J.; Thorp, H. H. *J. Am. Chem. Soc.* **2006**, *128*, 11020.
(36) Sjödin, M.; Irebo, T.; Utas, J. E.; Lind, J.; Merényi, G.; Åkermark, B.; Hammarström, L. *J. Am. Chem. Soc.* **2006**, *128*, 13076.
(37) Hodgkiss, J. M.; Rosenthal J.; Nocera, D. G. In *Handbook of Hydrogen Transfer*. *Physical and Chemical Aspects of Hydrogen Transfer*; Hynes, J. T., Klinman, J. P., Limbach, H.-H., Schowen, R. L., Eds.; Wiley-VCH: Weinheim, Germany, 2006; Vol. II, Part IV, Chapter 17, p 503.
(38) Ledger, M. B.; Porter, G. *J. Chem. Soc., Faraday Trans. 1* **1972**, *68*, 539.
(39) Clark, K. P.; Stonehill, H. I. *J. Chem. Soc., Faraday Trans. 1* **1972**, *68*, 577.
(40) Clark, K. P.; Stonehill, H. I. *J. Chem. Soc., Faraday Trans. 1* **1972**, *68*, 1676.
(41) Loeff, I.; Treinin, A.; Linschitz, H. *J. Phys. Chem.* **1983**, *87*, 2536.
(42) Adams, G. E.; Willson, R. L. *J. Chem. Soc., Faraday Trans. I* **1973**, *69*, 719.
(43) Lathioor, E. C.; Leigh, W. J.; St. Pierre, M. J. *J. Am. Chem. Soc.* **1999**, *121*, 11984.
(44) Seyedsayamdost, M. R.; Reece, S. Y.; Nocera, D. G.; Stubbe, J. *J. Am. Chem. Soc.* **2006**, *128*, 1569.
(45) Salowe, S.; Bollinger, J. M., Jr.; Ator, M.; Stubbe, J.; McCraken, J.; Peisach, J.; Samano, M. C.; Robins, M. J. *Biochemistry* **1993**, *32*, 12749.

chloride and loaded onto a Chromatotron plate (Si gel, 2 mm). The product was eluted with 2% MeOH/CH_2Cl_2. The solvent was removed in vacuo to yield a yellow oil, which was redissolved in 10 mL of 1:1 TFA/CH_2Cl_2 and stirred for 1 h. The solution was concentrated to <1 mL under a stream of N_2 and taken up in ether. The resulting yellow precipitate was isolated by filtration and dried in vacuo to yield 500 mg of the title compound as a yellow powder (95%). ^{1}H NMR (300 MHz, CD_3OD, 25 °C) δ = 3.05 (m, 1H, C_β−H), 3.26 (m, 1H, C_β−H), 4.83 (m, 1H, C_α−H), 6.72 (m, 2H, phenol-H), 7.13 (m, 2H, phenol-H), 7.85 (m, 2H, Anq arom C−H), 7.97 (m, 1H, N−H), 8.12 (m, 1H, Anq arom C−H), 8.27 (m, 3H, Anq arom C−H), 8.58 (d, 1H, N−H, 1.6 Hz). ESI-MS Calcd (Found): $[M + H]^+$ 416.11 (416.11), $[2M + H]^+$ 831.22 (831.21).

***N*-[(9,10-Dihydro-9,10-dioxo-2-anthracenyl)carbonyl]-L-phenylalanine (Anq-F-OH).** The title compound was prepared by the same method as that used for Anq-Y-OH, except that F-O*t*Bu·HCl was used in place of Y-O*t*Bu (63%). ^{1}H NMR (300 MHz, $(CD_3)_2CO$, 25 °C) δ = 3.14, (m, 1H, C_β−H), 3.40 (m, 1H, C_β−H), 4.93 (m, 1H, C_α−H), 7.17−7.35 (m, 5H, phenyl C−H), 7.87 (m, 2H, Anq arom C−H), 8.11 (m, 1H, Anq arom C−H), 8.29 (m, 3H, Anq arom C−H), 8.58 (d, 1H, Anq arom C−H, 1.6 Hz), 9.00 (d, 1H, N−H, 8.3 Hz). ESI-MS Calcd (Found): $[M + H]^+$ 400.12 (400.12), $[2M + H]^+$ 799.23 (799.22)

Synthesis of Chromophore-(Y/F)LVGQIDSEVDTDDLSNFQL [Chromophore-(Y/F)-R2C19]. Solid-phase peptide synthesis (SPPS) using Fmoc-protected amino acids was employed to extend the Fmoc-R2C19-PEG-PS resin-bound peptide, which was available from a previous study.[46] For the syntheses of the chromophore-(Y/F)-R2C19 peptides, typically 125 mg of the Fmoc-R2C19-PEG-PS resin-bound peptide (0.2 mmol/g) was loaded into a 10 mL Bio-Rad Poly-Prep column containing a porous 30 μm polyethylene bed in the bottom to hold the resin. The N-terminal Fmoc protecting group was cleaved by shaking the resin in a solution of 1.8 mL of 0.1 M HOBt in 20% piperidine/DMF for 3 × 8 min using a Fisher Scientific Vortex Genie 2 (VWR). The resin was then washed with 3 × 2 mL of DMF and CH_2Cl_2. Fmoc-Y(*t*Bu)-OH/Fmoc-F-OH was then coupled to the free N-terminus by shaking the resin for 2 × 70−80 min in a solution of 0.5 M amino acid, 0.45 M HATU, and 1 M DIPEA; the volume was adjusted accordingly such that the amino acid was in 6−8-fold excess. The chromophore-COOH (chromophore = Anq and Fmoc-BPA) compounds were then coupled in a similar manner with the following modifications. In the case of the Anq chromophore, the coupling solution consisted of 4 equiv of Anq-COOH suspended/dissolved in 300−600 μL of DMF containing 0.45 M HATU and 1 M DIPEA due to limited solubility of the chromophore. In the case of Fmoc-BPA, after chromophore coupling, the Fmoc protecting group was cleaved as described above and the N-terminus acetylated by shaking the resin in a 0.5 M acetic anhydride and 0.5 M DIPEA in DMF for 1 h. Cleavage of the peptide from the resin was carried out by shaking in 2.5 mL of 95% TFA, 2.5% triisopropylsilane, and 2.5% water for 4 h. The resin was then washed for 2 × 1 min with 2 mL of TFA. The cleavage cocktail and washings were combined, evaporated under a stream of N_2, and taken up in 15 mL of ether to precipitate the crude peptide, which was pelleted in a centrifuge and the ether decanted. The precipitate was dissolved in 0.1 M ammonium bicarbonate HPLC buffer via sonication over several minutes.

Peptide Purification and Characterization. Peptides were purified by reversed phase HPLC as previously described.[29] The HPLC system consisted of a Waters 600 controller and a Waters 996 photodiode array detector, which were interfaced to and controlled by a computer using Waters' Millenium 32 software. Samples were manually injected onto a semipreparative Waters XTerra MS C-18 column (19 × 100 mm), which had been previously equilibrated with 10% acetonitrile/0.1 M ammonium bicarbonate (pH 8). A linear gradient of 10% → 65% acetonitrile vs ammonium bicarbonate over 45 min at a flow rate of 5 mL/min was used to elute the peptides. The eluant absorbance was monitored at the λ_{max} of the chromophore and at 210 nm, where the peptide amide bond absorbs. Fractions were collected by hand, lyophilized, taken up in 50 mM Tris buffer at pH 7.5, combined, and stored at −80 °C. Analytical HPLC was employed to confirm the purity of the peptides. The samples were manually injected onto an analytical Waters XTerra MS C-8 (4.6 × 100 mm) column and eluted with the same gradient used for purification at a flow rate of 1 mL/min. The molecular weight (MW) of the peptide was characterized by MALDI-TOF mass spectrometry as described below. The HPLC retention times (t_R) and MALDI-TOF *m*/*z* ratios for each peptide are listed in Table 1. Analytical HPLC traces for each peptide recorded at 210 nm are shown in the Supporting Information (Figures S1−S4).

Table 1. Characterization of Peptides

peptide	t_R (min)[a]	MW calcd (*m*/*z*)	MW found (*m*/*z*)[b]	IC_{50}[c] (μM)
Ac-BPA-Y-R2C19	16.7	2563	2564	15
Ac-BPA-F-R2C19	18.3	2547	2548	30
Anq-Y-R2C19	17.1	2504	2507	4
Anq-F-R2C19	19.9	2488	2489	7

[a] Retention time (t_R) from analytical HPLC trace. Individual chromatograms are available in the Supporting Information. [b] MALDI-TOF MS in negative-ion mode. [c] Concentration of peptide at 50% RNR inhibition.

Isolation, Purification, and Prereduction of α2. *E. coli* α2 was isolated by standard procedures.[45] To remove contaminating β2, it was further purified using a POROS HQ/20 anion-exchange column (Applied Biosystems) on a BIOCAD Sprint Perfusion Chromatography System (Applied Biosystems). The column was loaded with α2 (10−15 mg) and washed with Tris buffer (50 mM, pH 7.6) for 5 min. α2 was eluted with a linear gradient of 0−700 mM NaCl over 30 min at a flow rate of 4 mL/min. Fractions were collected by hand and concentrated on a YM-30 membrane (Millipore). This procedure reduced background turnover of CDP 7−8 fold. To prereduce α2, ∼30 mg was incubated with 30 mM DTT for 30 min at room temperature. Hydroxyurea, ATP, and CDP were added to final concentrations of 30, 3, and 1 mM, respectively, and the incubation was continued for an additional 20 min. Another 10 mM DTT was added, and the mixture was incubated for 10 min and desalted on a G-25 Sephadex column (∼35 mL, 1.5 × 23 cm) pre-equilibrated in 50 mM Tris, 15 mM $MgSO_4$, pH 7.6.

α2 Activity Assay and Competitive Inhibition Assay for Binding of Peptide to α2. α2 (0.1 μM, specific activity = 1900 nmol min^{-1} mg^{-1}), β2 (0.2 μM, specific activity = 6800 nmol min^{-1} mg^{-1}), TR (30 μM), TRR (0.5 μM), NADPH (0.2 mM), CDP (1 mM), and ATP (1.6 mM) were combined in 50 mM HEPES, 15 mM $MgSO_4$, 1 mM EDTA buffer at pH 7.6. Enzyme activity was measured by consumption of NADPH, which was monitored by the decrease in absorbance at 340 nm. This was then repeated with peptide concentrations ranging from 2 to 80 μM.

Single-Turnover Assays for Photoinitiated Nucleotide Reduction in Peptide-α2 Complexes. The assays were performed by a method modified from that previously reported.[29] FPLC purified, prereduced α2 (20 μM, specific activity = 1800 nmol min^{-1} mg^{-1}), peptide (200 μM), ATP (3.0 mM), and [2-^{14}C]-CDP (1.0 mM, 5445 cpm nmol^{-1}) in 50 mM Tris, ∼7 mM $MgSO_4$ buffer at pH 7.5 were added to a 1 cm quartz microcuvette with a total solution volume of 200 μL. Care should be taken in preparation of the peptide stock solutions as they are sensitive to the concentration of $MgSO_4$ and the peptide can precipitate upon addition of solid $MgSO_4$ to the solutions. Typically, the peptide stock solutions were prepared in 50 mM Tris buffer (pH 7.5) and diluted into the reaction mixture containing millimolar concentrations of Mg^{2+}. The reaction was initiated by addition of [2-^{14}C]-CDP (97 mM), quickly mixed, spun down in a minicentrifuge (<10 s, 2000*g*) to consolidate the liquid, and pipetted into the cuvette. Samples were irradiated at room temperature with the focused light

(46) Yee, C. S.; Seyedsayamdost, M. R.; Chang, M. C. Y.; Nocera, D. G.; Stubbe, J. *Biochemistry* **2003**, *42*, 14541.

from a 1000 W Xe arc lamp equipped with 299 nm long-pass and IR filters. Fractions (60 μL) were removed at 2, 5, and 10 min intervals and immediately quenched by heating in a boiling water bath for 2 min. The precipitated protein was then spun down for 10 min in a minicentrifuge at 20 000*g*. The supernatant (50 of the 60 μL) was transferred to a new Eppendorf tube, diluted with 14 units of alkaline phosphatase and 120 nmol of carrier dC to a final volume of 170 μL, and incubated at 37 °C for 2 h in a sealed Eppendorf vial. dC was then separated from C and quantitated as previously described.[47,48] Each reaction was repeated twice along with a dark α2 control and a dark α2-peptide control to quantify background counts arising from contaminating β2 that co-purifies with α2 and from radiochemical impurities in the stock [2-^{14}C]-CDP that elute with the product. Background counts were low in these experiments, as shown in Table S1. For reactions involving the Y730F-α2 mutant, 90 μM peptide and 20 μM protein were used with all other conditions the same as for wt-α2.

Physical Measurements. ^{1}H NMR spectra were recorded on a Varian Mercury 300 MHz NMR at the MIT Department of Chemistry Instrumentation Facility (DCIF) and externally referenced to tetramethylsilane. ESI-FT mass spectrometry was performed with a Brüker Daltonics APEXII instrument housed in the DCIF. MALDI-TOF mass spectrometry was performed with a Brüker Omniflex instrument in the DCIF using α-cyano-4-hydroxycinnamic acid as the matrix. The instrument was calibrated in positive-ion mode with a quadratic polynomial using a mixture of angiotensin II (1046.5423), P14R synthetic peptide (1533.8582), and ACTH fragment 18−39 (2465.1989) (Sigma). All peptides synthesized were analyzed in negative-ion mode due to the large number of carboxylate-containing residues.

UV−vis absorption spectra were recorded on a Cary 17D modified by On-Line Instrument Systems (OLIS) to include computer control or a Spectral Instruments 440 spectrophotometer. TA measurements were made with pump light provided by the third harmonic (355 nm) of an Infinity Nd:YAG laser (Coherent) running at 20 Hz as previously described.[49] In the case of the BPA, 300 nm pump light was used as previously described owing to the lack of absorption at 355 nm for this chromophore.[44] Transient absorption experiments for all compounds were performed in a 2 mm cuvette in 20 mM Tris buffer at pH 7.5 at 350 μM for Anq dipeptides/Y(F)-R2C19 peptides and 500 μM for the BPA dipeptides/Y-R2C19 peptide. Sample volumes of 200 μL were employed for all peptide spectroscopy experiments reported herein. For transient absorption experiments involving Anq-Y-OH, 10 mL of solution was continuously flowed through a 2 mm cuvette during data collection to ensure that fresh sample was present for each laser shot. All experiments were performed under ambient conditions.

Results

Synthesis. Dipeptides containing the chromophore and Y or F were synthesized and their photoreactions examined by TA spectroscopy. The efficacy of the BPA and Anq chromophores as competent photo-oxidants of Y is more conveniently established with the dipeptides as opposed to full-length R2C19 peptide since the former are more readily synthesized and offer a simplified photochemistry by avoiding potential side reactions of the chromophore excited states with other residues on R2C19. The BPA-Y-OMe dipeptide synthesis and TA spectroscopy have been reported previously.[44] The Anq dipeptides are furnished by coupling the carboxylic-acid-containing Anq-COOH chromophore to the primary amine of the *tert*-butyl-ester-protected amino acid (F-O*t*Bu and Y-O*t*Bu) using standard peptide coupling conditions. The *tert*-butyl ester of the amino acid was removed with TFA to yield the free carboxylic acid, thereby improving water solubility of the dipeptide. The UV−vis ground-state absorption spectra of BPA-Y-OMe·TFA and Anq-Y-OH are shown Figure 3; Anq-Y-OH has a much larger absorption cross section outside of the protein absorption envelope.

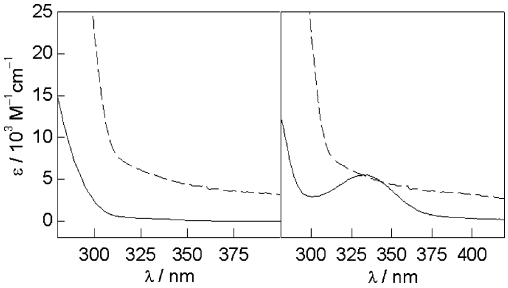

Figure 3. Ground-state UV−vis absorption spectra of BPA-Y-OMe (—, left) and Anq-Y-OH (—, right). Overlaid in both spectra is the absorption spectrum of α2 (- -). The estimated extinction coefficients for BPA-Y-OMe, Anq-Y-OH, and α2 are 2300, 2900, and 22000 M^{-1} cm^{-1} at 300 nm and ~50, 2600, and 4200 M^{-1} cm^{-1} at 355 nm, respectively.

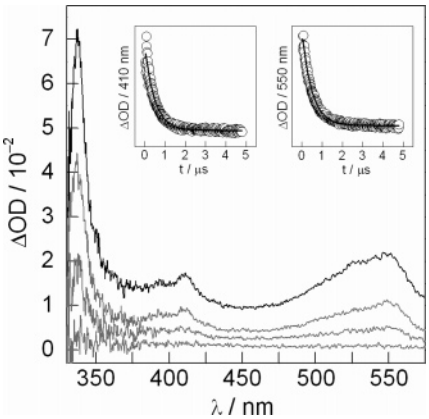

Figure 4. Transient absorption spectra of BPA-Y-R2C19 obtained 65 ns, 415 ns, 1, and 10 μs (—) following 300 nm excitation. (Insets) Time-evolved absorbance data (○) with monoexponential decay fit (—) obtained at 410 and 550 nm.

Chromophore-(F/Y)-R2C19 peptides were synthesized by extending the Fmoc-R2C19-PEG-PS resin-bound peptide, first with Fmoc-(F/Y)-OH followed by the appropriate carboxylic-acid-containing chromophore (Fmoc-BPA-COOH or Anq-COOH) using standard Fmoc-SPPS conditions. Table 1 lists the HPLC retention times and MALDI-TOF mass spectral data for each of the peptides synthesized. Analytical HPLC traces, obtained by monitoring the absorbance at 210 nm, were used to characterize peptide purity and are provided for each peptide in Figures S1−S4.

Time-Resolved Spectroscopy. The BPA and Anq dipeptides and full-length peptides were weakly emissive or nonemissive in aqueous solutions. Accordingly, formation and reaction of the chromophore excited states and photoproducts were characterized by transient absorption spectroscopy.

The BPA-Y-OMe dipeptide produces the $^{\bullet}$BPA-Y$^{\bullet}$-OMe diradical state upon excitation with λ_{exc} = 300 nm. Radical recombination occurs with a rate constant of 5.6×10^6 s^{-1}.[44] The transient absorption and kinetics traces shown in Figure 4 establish a similar photochemistry for the full-length peptide, Ac-BPA-Y-R2C19. Transient absorption features at 337, 410, and 550 nm, obtained 65 ns following 300 nm excitation, are

(47) Steeper, J. R.; Steuart, C. D. *Anal. Biochem.* **1970**, *34*, 123.
(48) Booker, S.; Licht, S.; Broderick, J.; Stubbe, J. *Biochemistry* **1994**, *33*, 12676.
(49) Loh, Z.-H.; Miller, S. E.; Chang, C. J.; Carpenter, S. D.; Nocera, D. G. *J. Phys. Chem. A* **2002**, *106*, 11700.

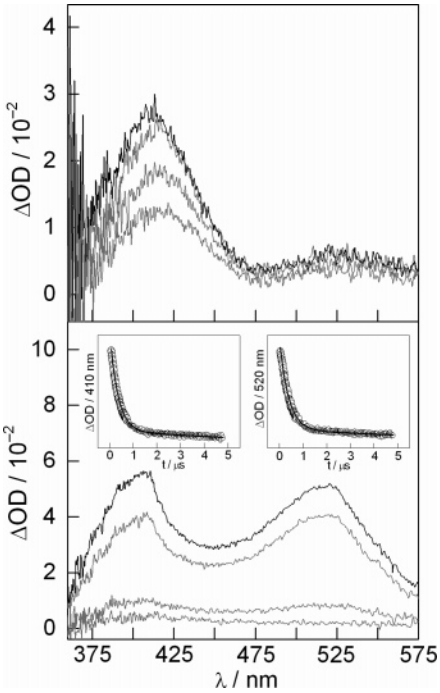

Figure 5. (Top) Transient absorption spectra of Anq-F-OH obtained 65 ns, 115 ns, 1, and 10 μs (—) following 355 nm excitation. (Bottom) Transient absorption spectra of Anq-Y-OH obtained 15 ns, 115 ns, 1 μs, and 10 μs (—) following 355 nm excitation. (Insets) Time-evolved absorbance data (○) with biexponential decay fit (—) obtained at 410 and 520 nm.

consistent with formation of Y$^\bullet$ ($\epsilon_{410\,nm} = 2750 \pm 200$)[50] and the benzophenone radical ($\epsilon_{330\,nm} = 22\,000\ M^{-1}\ cm^{-1}$ and $\epsilon_{540\,nm} = 2800\ M^{-1}\ cm^{-1}$).[42] The triplet of benzophenone is formed with a quantum yield near unity and persists on the microsecond time scale in water.[51] Thus, we can estimate a near unity quantum yield for formation of the $^\bullet$BPA-Y$^\bullet$ diradical state. The overall absorption profile does not change over the time course of 415 ns, 1 μs, and 10 μs. Time-evolved absorption kinetics obtained at 410 and 550 nm (inset of Figure 4) can both be fit to a monoexponential decay function with a time constant of 490 $\pm$ 20 ns, thus yielding a rate constant for radical recombination of $2.0 \pm 0.1 \times 10^6\ s^{-1}$. The direct and concomitant return of the transient signals of $^\bullet$BPA and $^\bullet$Y to baseline indicates that radical recombination proceeds without production of additional intermediates. Moreover, the similarity of the transient data for the dipeptide and full-length peptide indicates that the BPA reacts solely with Y and not other residues on the R2C19 peptide.

The photochemistry of Anq-derivatized dipeptide is more complex. The triplet excited state of 9,10-anthraquinone-2-sulfonate, ^{3}AQS, is known to react with water and/or OH^-, although the exact photoproducts and reaction mechanism are ill defined.[41] Accordingly, the TA spectra of Anq-F-OH were used as a control and compared to that for Anq-Y-OH to distinguish the spectra of the Anq excited state and/or side photoproducts from the products of tyrosine oxidation. Figure 5 (top) shows the absorption spectrum obtained 50 ns after Anq-F-OH dipeptide was excited with a 355 nm nanosecond laser pulse. The transient contains a broad feature with $\lambda_{max} \approx$ 417 nm and an even broader and weaker shoulder with $\lambda_{max} \approx$ 530 nm. Additional spectra obtained at 100 ns, 1 μs, and 10 μs show that the overall profile is invariant with time. Analysis of the single-wavelength kinetics at 410 nm reveals a nonexponential decay, which does not return to baseline on the microsecond to millisecond timescale. This long-lived process is not a result of a photoreaction with the buffer, as similar spectra and kinetics were recorded when Tris buffer (pH 7.6) was employed. In light of these results together with the absence of observable triplet phosphorescence, which is normally observed for ^{3}Anq in organic solvents, the spectrum in the top panel of Figure 5 likely arises from a photoreaction between ^{3}Anq and water.

The bottom panel of Figure 5 displays the results for a transient experiment performed on Anq-Y-OH under the identical set of experimental conditions employed for Anq-F-OH. The first transient (50 ns) is markedly different from that obtained for Anq-F-OH and contains features with $\lambda_{max} \approx$ 520 and 410 nm and a shoulder at 395 nm. We ascribe the 520 nm absorption to the anthraquinone semiquinone radical anion, Anq$^{\bullet-}$, based on similar absorption spectra to that of the native 9,10-anthraquinone semiquinone radical anion ($\epsilon_{395} = 7800\ M^{-1}\ cm^{-1}$ and $\epsilon_{480} = 7300\ M^{-1}\ cm^{-1}$ at p$K_a = 5.3$)[52] and anthraquinone-2-sulfonate semiquinone radical anion ($\epsilon_{400} = 8000\ M^{-1}\ cm^{-1}$, $\epsilon_{500} = 8000\ M^{-1}\ cm^{-1}$ at p$K_a = 3.25$).[53] The higher energy TA band is a superposition of two absorptions at 394 and 408 nm; these wavelengths are commensurate with the absorptions of Y$^\bullet$ ($\epsilon_{410\,nm} = 2750 \pm 200$)[50] and Anq$^{\bullet-}$ of the diradical, Anq$^{\bullet-}$-Y$^\bullet$-OH, which we propose to result from Y oxidation by the triplet nπ^* excited state of Anq, ^{3}Anq. This photochemistry is consistent with the known reactivity of ^{3}Anq with alcohols.[54,55] The concomitant disappearance of the 410 and 520 nm transient absorptions (Figure 5, bottom) are indicative of radical recombination. A small residual absorbance, evident at times >10 μs, is similar to the transient features observed with Anq-F-OH (Figure 5, top). Single-wavelength kinetics obtained at 410 and 520 nm are best fit to a biexponential decay function with short ($\tau_1 = 370 \pm 20$ ns, 80%) and long ($\tau_2 >$ 10 μs, 20%) components. The major, short component of the decay is assigned to radical recombination between Anq$^{\bullet-}$ and Y$^\bullet$ in Anq$^{\bullet-}$-Y$^\bullet$-OH, proceeding at $2.7 \pm 0.1 \times 10^6\ s^{-1}$. The minor, long component is assigned to the decay of the Anq−solvent photoproduct identified in the TA spectrum of the Anq-F-OH dipeptide (vide supra).

Against the backdrop of these dipeptide results, the TA spectroscopy for Y$^\bullet$ generation in Anq-Y-R2C19 peptide was investigated. Figure 6 (top) shows the transients obtained 100 ns, 1 μs, and 10 μs after excitation of Anq-Y-R2C19 with a 355 nm laser pulse. The spectra are similar to those observed for the Anq-Y-OH dipeptide and are ascribed to the Anq$^{\bullet-}$-Y$^\bullet$-R2C19 diradical state of the peptide. Single-wavelength kinetics obtained at 410 and 520 nm (Figure 6, left and right insets) could be fit to a biexponential decay with short, major and long, minor components similar to that for Anq-Y-OH: 410 nm, $\tau_1 = 540 \pm 30$ ns (80%), $\tau_2 = 2.1 \pm 0.3$ μs (20%); 510 nm, $\tau_1 = 630 \pm 70$ ns (80%), $\tau_2 = 2.1 \pm 0.3$ μs (20%). The shorter components are the same within the error of the measurement and, as with Anq-Y-OH, attributed to radical recombination

(50) Feitelson, J.; Hayon, E. *J. Phys. Chem.* **1973**, *77*, 10.
(51) Canonica, S.; Hellrung, B.; Wirz, J. *J. Phys. Chem. A* **2000**, *104*, 1226.
(52) Rao, P. S.; Hayon, E. *J. Phys. Chem.* **1973**, *77*, 2274.
(53) Hulme, B. E.; Land, E. J.; Phillips, G. O. *J. Chem. Soc., Faraday Trans. 1* **1972**, *68*, 1992.
(54) Carlson, S. A.; Hercules, D. M. *Photochem. Photobiol.* **1973**, *17*, 123.
(55) Görner, H. *Photochem. Photobiol.* **2003**, *77*, 171.

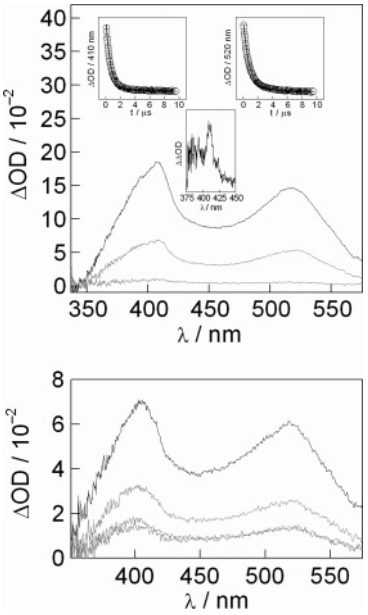

Figure 6. (Top) Transient absorption spectra of Anq-Y-R2C19 obtained 115 ns, 1 μs, and 10 μs (—) following 355 nm excitation. (Left and right insets) Single-wavelength kinetics traces (○) with biexponential decay fit (—). (Middle inset) Plot of ΔΔOD obtained by subtracting the normalized transients observed for Anq-Y-R2C19 and Anq-F-R2C19 at 100 ns. (Bottom) Transient absorption spectra of Anq-F-R2C19 obtained 115 ns, 1 μs, 10 μs, and 100 μs (—) following 355 nm excitation.

between $Anq^{\bullet-}$ and $Y^{\bullet}$ on the peptide with a rate constant of $1.7 \pm 0.3 \times 10^6\ s^{-1}$. As with Anq-Y-OH, we attribute the slower component to the decay of the Anq−solvent photoproduct.

To further confirm $Y^{\bullet}$ formation in Anq-Y-R2C19, the control peptide Anq-F-R2C19 (as with the dipeptides) was examined in an effort to uncover photochemical reactivity arising from something other than Y356 as a number of other residues are potential reductants of ^{3}Anq. ^{3}AQS has been shown to oxidize the carboxylate-containing residues of glycyl−glycine dipeptides leading to formation of the $AQS^{\bullet-}$ semiquinone anion radical and the decarboxylated amidomethylene radical.[56,57] There are five carboxylic-acid-containing Asp/Glu residues on the R2C19 peptide. In addition, ^{3}Anq has also been shown to oxidize alcohols;[54] both hydroxyl-containing Ser and Thr residues are present on R2C19 as well. The bottom panel of Figure 6 shows the transients observed upon excitation of the Anq-F-R2C19 peptide with 355 nm excitation at 100 ns, 1 μs, 10 μs, and 100 μs. These transients observed at 100 ns do not resemble that for Anq-F-OH (Figure 5, top). The peaks at 410 and 520 nm resemble that of $Anq^{\bullet-}$. The decay of the signals at 410 and 520 nm in the bottom panel of Figure 6 is complex, decaying on both the hundreds of nanoseconds and microsecond timescales, with an $Anq^{\bullet-}$ remaining after 100 μs. Because $Anq^{\bullet-}$ should be the only absorbing species in the 375−450 nm spectral region upon excitation of Anq-F-R2C19, this spectrum may be used for normalization and subtraction of the transients following excitation of Anq-Y-R2C19 and Anq-F-R2C19 at 100 ns. The inset in the top of Figure 6 (middle inset) plots ΔΔOD for this subtraction. The distinctive $Y^{\bullet}$ absorption profile, with at peak at 410 nm and a shoulder to the blue (for reference, compare to Figure 4 with the Ac-BPA-Y-R2C19 system), is obtained. This difference spectrum further supports the contention that $Y^{\bullet}$ is produced promptly after excitation of Anq-Y-R2C19.

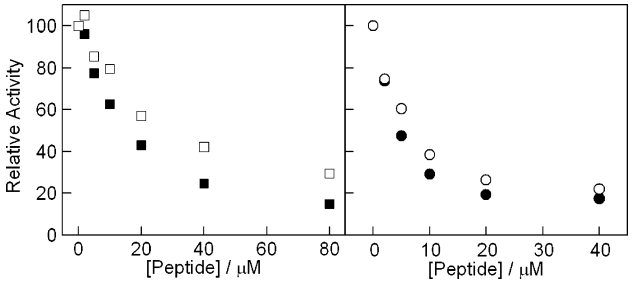

Figure 7. Plots of relative RNR activity vs peptide concentration in the competitive inhibition binding assay for Ac-BPA-Y-R2C19 (■), Ac-BPA-F-R2C19 (□), Anq-Y-R2C19 (●), and Anq-F-R2C19 (○) peptides.

Peptide Binding to α2. To study PCET in α2 by the approach in Figure 2, the chromophore-(Y/F)-R2C19 peptides need to bind to α2. A protocol has been developed by Climent and co-workers[27,28] to assess binding of β2 C-terminal tail peptides of various lengths to α2. These studies found that (1) the C-terminal peptide tail of β2 accounts for most of the binding interaction between this subunit and α2, (2) these peptides are inhibitors of RNR activity by competing with β2 for binding to α2, (3) addition of an N-terminal tyrosine to Ac-R2C19 to form Ac-Y-R2C19 results in stronger binding by a factor of 2 (K_i = 40.0 and 20.0 μM, respectively), and (4) further addition of residues at the N-terminus, up to R2C37, did not significantly enhance binding. We were interested in knowing whether addition of a chromophore to the N-terminus of Y-R2C19 significantly perturbs binding from that of the native peptide studies of Climent. To address this issue we used Climent's methods[27] to assess binding of the Ac-BPA- and Anq-containing peptides.

α2 and β2 (0.1 and 0.2 μM, respectively) were combined, and the relative RNR activity was measured as the peptide concentration was increased from 0 to 80 μM. Under these conditions the peptide concentrations at 50% inhibition, IC_{50}, can be used to approximate K_i.[27] IC_{50}s were estimated from the plots of relative RNR activity vs peptide concentration shown in Figure 7 and are listed in Table 1. These data show that the presence of the chromophore does not weaken binding. In fact, the Anq-containing peptides bind more strongly by a factor of ~4 compared to the BPA-containing peptides, suggesting a hydrophobic interaction between the planar aromatic chromophore and the surface of α2. Furthermore, replacement of the F residue with Y at position 356 on peptides *of the same length* results in a doubling of the binding strength, suggesting a specific interaction between the hydroxyl group of Y356 and residues in α2.

Photoinitiated Nucleotide Reduction. Having established the $Y^{\bullet}$ photogeneration and α2 binding, light-initiated nucleotide reduction assays were examined to test whether charge transport occurs across the noncovalent peptide/α2 complex. To quantitate the maximum amount of dCDP that could be formed under single-turnover conditions, α2 was incubated with β2 and CDP substrate for 10 min. To determine if the peptide deactivates the enzyme in the dark, α2 was also incubated with the Ac-BPA-Y-R2C19 peptide in the dark for 2 min followed by 10 min incubation with β2 and CDP substrate. Both experiments resulted in 2.1 equiv of dC per dimer of α2 (Table S1); the

(56) Tarábek, P.; Bonifačić, M.; Beckert, D. *J. Phys. Chem. A* **2004**, *108*, 3467.
(57) White, R. C.; Tarasov, V. F.; Forbes, M. D. E. *Langmuir* **2005**, *21*, 2721.

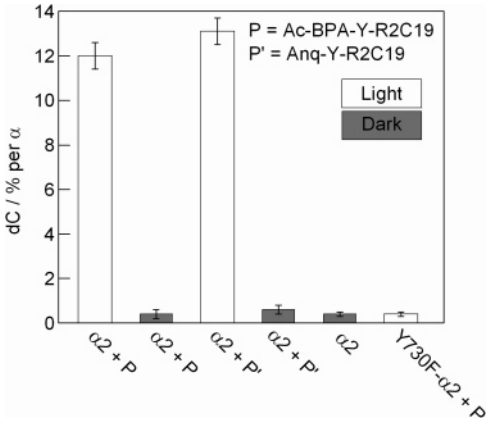

Figure 8. Light-initiated, single-turnover assays with Ac-BPA-(Y)-R2C19:α2, Anq-Y-R2C19:α2, and Ac-BPA-Y-R2C19:Y730F-α2. The bars refer to light (□) reactions and dark (■) controls. For 100% turnover, each dimer of α2 would produce two molecules of dCDP.

photoassay data are therefore reported as a percent turnover per equivalent of monomer, α.

Photoinitiated nucleotide reduction was performed under conditions where all α2 was bound to peptide. The calculation of the percent α2 bound treats the α2 dimer as two separate monomers that each bind one peptide with the same K_d. By following the protocol of Climent and co-workers,[27] the IC_{50} values in Table 1 may be used to approximate K_d for the peptide-α2 complex. Under the conditions of the single-turnover assays for photoinitiated CDP reduction, α2 is 92% and 98% bound by Ac-BPA-Y-R2C19 and Anq-Y-R2C19 peptides, respectively.

The results of the photoassay for α2:Ac-BPA-Y-R2C19 and α2:Anq-Y-R2C19 protein:peptide complexes are presented in Figure 8 and Table S1. Turnover for wt-α2 was complete by the time the first data point was collected (2 min), and therefore, data collected at subsequent times (i.e., 5 and 10 min) were invariant. Accordingly, the data for wt-α2 correspond to the average of nine data points (3 × 2, 5, and 10 min). The Ac-BPA-Y-R2C19 and Anq-Y-R2C19 peptides turnover α2 under irradiation at 12.0 ± 0.6% and 13.1 ± 0.6%, respectively (indicated by the open bars in Figure 8), which are well above the background turnover (gray bars) that arises from β2 contamination and radiochemical impurities. In an attempt to understand why turnover was limited to ∼13%, the activity of α2 was assayed before and after photolysis with the Ac-BPA-Y-R2C19 peptide. At 2 min, α2 photolyzed in the presence of peptide was found to be completely inactive for nucleotide reduction with β2 (Table S1), whereas the α2 from the dark reaction maintained activity up to the final time point of 10 min. SDS gels of the dark and light reactions (Figure S5) reveal that the α2 band from the light reaction smeared compared to the dark control, consistent with multiple cross links of the peptide to α2 and degradation of the protein. These data indicate that either the ^{3}BPA or radical photoproducts can deactivate the enzyme by direct reaction with α2.

The photoactivity of the α2:Ac-BPA-Y-R2C19 protein:peptide complex is perturbed significantly by replacement of Y730 with phenylalanine. Assuming that K_d for the Y730F-α2 peptide complex is the same as that with wt-α2, Y730F-α2 is 80% bound by the Ac-BPA-Y-R2C19 peptide under the conditions of the assay. However, the turnover measured for Y730F-α2 bound by Ac-BPA-Y-R2C19 after 2 min of photolysis is within the background levels of the assay (see Figure 8), indicating that the mutant is inactive toward photoinitiated dCDP production.

Discussion

The excited states of BPA and Anq are rapid ($>10^8$ s^{-1}) phototriggers of Y• when appended to the 20-mer peptide C-terminus of β2. The modified Y-R2C19 peptides bind to α2 with comparable or larger affinity than Y-R2C19 itself, suggesting a hydrophobic interaction between the chromophore and α2. Light excitation of the α2:X−Y-R2C19 (X = Ac-BPA or Anq) complex triggers RNR activity, as determined by single-turnover assays of α2 in the presence of substrate and effector. In this way, the entire β2 subunit of the Class I enzyme can be replaced by a small, redox-active peptide for •C439 radical generation in the active site in much the same way as β2 is replaced by the small adenosylcobalamin cofactor in the Class II RNR enzyme.[58]

The BPA and Anq add to the growing repertoire of Y• phototrigggers of RNR. Tryptophan may also effect light-initiated activity of RNR;[29] however, the process does not occur through a discrete excited state. W• radicals are obtained through irreversible photoionization of W, which leads to peptide decomposition.[30] The TA spectra shown in Figures 4 and 6 establish that Y• is transiently generated in BPA- and Anq-containing peptides and that the radical decays (τ = 500 ns lifetime) via charge recombination to reform the ground-state products. Thus, in the absence of α2, the peptide is stable to excitation. However, we note that benzophenone is commonly used as a photoactive cross linker for peptide and protein ligation.[59] Peptide cross linking to α2 would compete with Y oxidation on Y-R2C19 and may provide an explanation for the limiting turnover of 12−13%, which is comparable to that obtained with the W-based system.[29]

Radical transport from Y356 to C439 in the active site of α2 has been proposed to occur through Y731 and Y730 residues.[4] Y730F and Y731F-α2 site-directed mutants are inactive, and the hydrogen-bond network among Y730-Y731-C439 was accordingly proposed to be critical for radical transport in α2.[60] Photochemical radical generation by W on the Y-R2C19 peptide bound to α2 supports this contention.[29] The crystal structure of α2 (Figure 1) shows the Y731-Y730-C439 triad to be within hydrogen-bonding contact distances, with Y731 at the surface of α2.[17] The peptide region of β2 containing Y356 is particularly mobile in that it is not located in the crystal structure of β2 or in the structure of α2 with the Y-R2C19 peptide bound. Thus, the photo-oxidant or a mobile •Y356 residue photogenerated on the BPA/Anq-Y-R2C19 peptide bound to α2 could, in principle, interact with Y731. In either case, we can probe the mechanism of radical transport along the Y731-Y730-C439 pathway.

We consider three distinct mechanisms for radical transport in α2; these are summarized in Figure 9: (1) ET superexchange in which an electron tunnels from C439 to •Y731 directly; (2) ET hopping in which the electron hole tunnels from •Y731 →

(58) Sintchak, M. D.; Arjara, G.; Kellogg, B. A.; Stubbe, J.; Drennan, C. L. *Nat. Struct. Biol.* **2002**, *9*, 293.
(59) For example, see: Farrell, I. S.; Toroney, R.; Hazen, J. L.; Mehl, R. A.; Chin, J. W. *Nat. Methods* **2005**, *2*, 377.
(60) Ekberg, M.; Sahlin, M.; Eriksson, M.; Sjöberg, B.-M. *J. Biol. Chem.* **1996**, *271*, 20655.

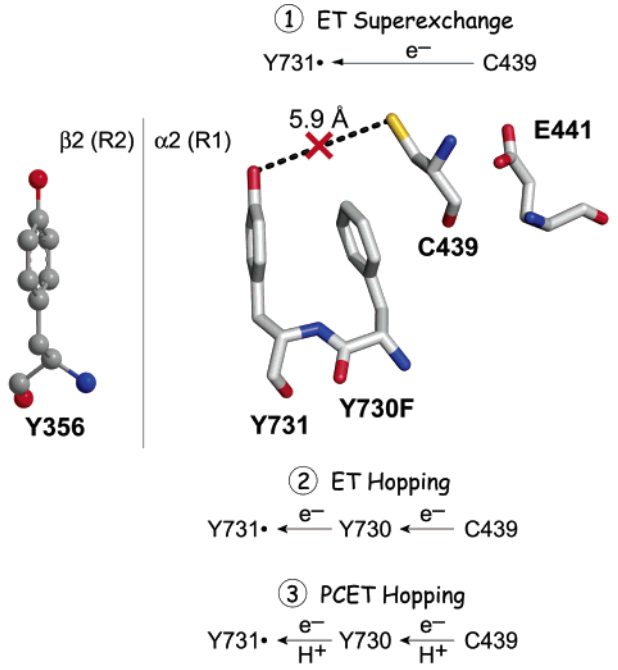

Figure 9. Crystal structure of the Y730F- α2 variant showing that mutation of Y730 to F interrupts the hydrogen-bond network in α2 and significantly increases the proton tunneling distance. Y356 on the R2C20 peptide is not located in the structure and is represented here for illustrative purposes.

Y730 → C439, forming the protonated $Y730^{\bullet+}$ radical cation as an intermediate; and (3) PCET hopping in which both an electron and a proton tunnel between the •Y731 → Y730 → C439 residues, forming the neutral •Y730 radical as an intermediate. The Y730F-α2 variant provides a convenient way to evaluate these potential mechanisms by independently tuning the electron- and proton-transfer distances. As described above, the X-ray crystal structure of the Y730F-α2 variant[61] (Figure 9) reveals that the mutation breaks the hydrogen-bond network between Y731 and C439 while maintaining the protein fold and the distance among the π systems of the aromatic rings.

The results of the Y730F-α2 mutant discount mechanism 1 as a possibility for radical transport. We contend that superexchange tunneling in this system should be mediated by the $\pi-\pi$ interaction between the aromatic Y731-Y730 residues rather than via the hydrogen-bond network as the latter provides a poor conductor of electronic coupling.[62,63] Disruption of the proton-transfer network should do little then to perturb a direct electron-transfer superexchange pathway since the distance between the aromatic residues is preserved. Accordingly, the rates for radical transport, and consequently turnover, would not be expected to differ greatly in wt-α2 or Y730F-α2. However, Figure 8 clearly shows that photoinitiated turnover (and thus radical transport) is perturbed in the mutant.

Mechanism 2 relies on ET hopping among aromatic residues, which can prevail for long-distance charge transfer in proteins[64,65] and DNA.[66] For this case, the "hop" in the Y730F mutant entails ET tunneling from C439 to Y731. The hopping distance increases by ~2.5 Å with the replacement of Y730 with phenylalanine. Using a $\beta = 1.1$ Å^{-1} for tunneling through a three-ring pathway,[67] the increased distance in Y730F-α2 should reduce the rate to ~6% that of wild-type (assuming all parameters equal except for distance). On the basis of this ET-hopping radical transport rate, an overall activity of 0.8% would be expected. From the data in Figure 8 and Table S1, turnover with Y730F-α2 is 0.4 ± 0.1%, which is less than that expected for a direct tunneling or hopping pathway. We note that the 0.1% error is the lower limit of our detection. As can be seen from the data for the α2 dark control experiment, the 0.4% activity includes counts from contaminating background radiation (most likely due to radiological impurities in CDP). If the activity is normalized to this background, the Y730F-α2 mutant is essentially inactive.

Of relevance to radical transport by mechanism 3, the self-exchange reaction between phenoxyl radical and phenol has recently been studied computationally.[68,69] The reaction occurs within a hydrogen-bonded complex and proceeds via a PCET mechanism in which the electron is transferred between orbitals of π symmetry on the phenol and the proton is transferred between distinct orbitals of σ(O−H) symmetry.[68,69] As discussed, since the electron and proton transport are of different origins, the PCET is not derived from a genuine hydrogen-atom transfer but rather from the coupling between the electron and proton.[37] Inasmuch as the electron and proton tunnel for such transfers, the reaction rates are predicted to be highly dependent on tunneling distance[69] and, as emphasized, the decoupling of electron-transfer and proton-transfer distances is crucial to probing PCET mechanisms.[1,37] The Y730F mutation increases the tunneling distance for the proton, assuming that crystallographically unidentified water molecules are not present in the structure, while maintaining the electron-transfer distance. The O−S distance from Y731 to C439 is 5.9 Å in Y730F-α2, while in wt-α2 the longest distance between phenol−O and thiol−S atoms is 3.4 Å. The attenuation of turnover is consistent with the interruption of the proton-transfer pathway, as diagrammatically indicated in Figure 9.

The foregoing analysis points toward a proton-dependent hopping mechanism for radical transport in α2. Higher turnover numbers with wt-α2 compared to that for Y730F-α2 will be critical to further distinguishing between ET (mechanism 2) and PCET (mechanism 3) hopping mechanisms. We note that the active RNR complex may be an asymmetric dimer,[22,70] and hence, the activity of the peptide-α2 may be limited to 50% owing to half-site reactivity in α2. To overcome this complication, we are now focusing on direct spectroscopic detection of radicals along the pathway in α2. To this end, the current BPA- and Anq-containing peptides set a benchmark inasmuch as Y• may be generated with excitation light that lies to the red spectral side of the protein absorption envelope, and for BPA, the Y• absorption feature can be clearly detected. The disadvantages

(61) Eriksson, M.; Uhlin, U.; Ramaswamy, S.; Ekberg, M.; Regnström, K.; Sjöberg, B.-M.; Eklund, H. *Structure* **1997**, *5*, 1077.
(62) Gray, H. B.; Winkler, J. R. *Q. Rev. Biophys.* **2003**, *36*, 341.
(63) Hodgkiss, J. M.; Damrauer, N. H.; Pressé, S.; Rosenthal, J.; Nocera, D. G. *J. Phys. Chem. B* **2006**, *110*, 18853.
(64) Belliston-Bittner, W.; Dunn, A. R.; Nguyen, Y. H. L.; Stuehr, D. J.; Winkler, J. R.; Gray, H. B. *J. Am. Chem. Soc.* **2005**, *127*, 15907.
(65) Aubert, C.; Vos, M. H.; Mathis, P.; Eker, A. P.; Brettel, K. *Nature* **2000**, *405*, 586.
(66) Lewis, F. D. In *Electron Transfer in Chemistry*; Balzani, V., Ed.; Wiley-VCH: Weinheim, Germany, 2001; Vol. 3, Part 1, Chapter 5, p 105.
(67) Lee, M.; Shephard, M. J.; Risser, S. M.; Priyadarshy, S.; Paddon-Row, M. N.; Beratan, D. N. *J. Phys. Chem. A* **2000**, *104*, 7593.
(68) Mayer, J. M.; Hrovat, D. A.; Thomas, J. L.; Borden, W. T. *J. Am. Chem. Soc.* **2002**, *124*, 11142.
(69) Skone, J. H.; Soudackov, A. V.; Hammes-Schiffer, S. *J. Am. Chem. Soc.* **2006**, *128*, 16655.
(70) Seyedsayamdost, M. R.; Stubbe, J. *J. Am. Chem. Soc.* **2007**, *129*, 2226.

of the BPA and Anq chromophores lie in their complicated photochemistry and propensity toward protein cross linking/degradation. Future experiments will take advantage of the lower energy metal-to-ligand charge-transfer excited states of metal complexes[31] that are competent for radical generation in conjunction with fluorotyrosine unnatural amino acids.[44,71] Implementation of the approach described here with these modified peptide constructs is underway.

(71) Reece, S. Y.; Seyedsayamdost, M. R.; Stubbe, J.; Nocera, D. G. *J. Am. Chem. Soc.* **2006**, *128*, 13654.

Acknowledgment. Financial support for this research was provided by the National Institutes of Health (GM47274 (D.G.N.) and GM29595 (J.S.)).

Supporting Information Available: Analytical HPLC chromatograms for each peptide synthesized herein; SDS gel analysis of pre- and post- photolyzed Ac-BPA-YR2C19:α2 complexes; and, single turnover photoinitiated CDP reduction assay data in tabular form. This material is available free of charge via the Internet at http://pubs.acs.org.

JA0704434